The SAR values are calculated when the feeding point met the grid point of the scanning area by following definition:

$$\mathrm{SAR} = \frac{\sigma}{\rho} E^2 \quad [\mathrm{W/kg}] \tag{1}$$

where σ is the conductivity of the biological tissue [S/m], ρ is the density of the biological tissue [kg/m^3], and E is the electric field (rms) [V/m]. In order to calculate the SAR values in each position, finite-difference time-domain (FDTD) method [7] was employed. Table 1 shows parameters for FDTD calculations.

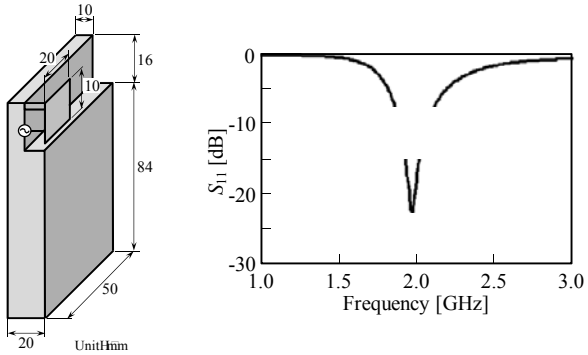

Figure 3. Mobile radio terminal model.

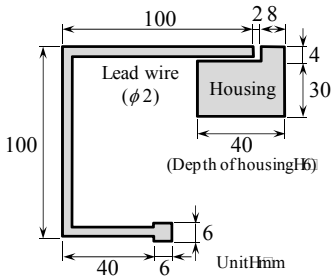

Figure 4. Pacemaker model.

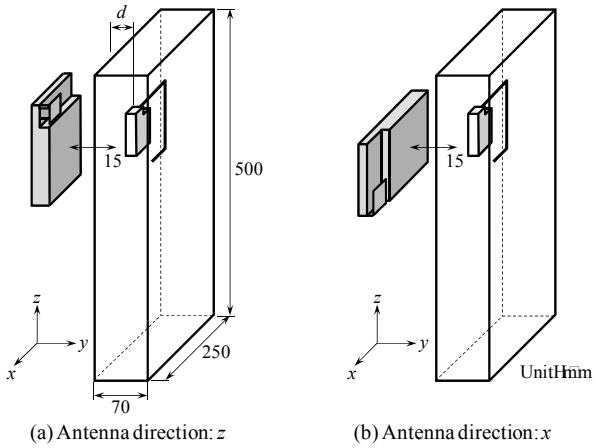

(a) Antenna direction: z (b) Antenna direction: x

Figure 5. Arrangements of torso model and mobile radio terminal model.

III. Calculated Results

Figure 7 shows the calculated 10-g averaged SAR in the scanning area, when depth of the pacemaker model d =14 mm. From Fig. 7(a), maximum 10-g averaged SAR appears on the origin of scanning area, in the antenna direction z. On the other hand, in Fig. 7(b), the maximum 10-g averaged SAR is observed at x =10 mm, z =-30 mm. This is a position that the lead wire of x-direction (longer part) overlapped almost center of the metallic case of mobile radio terminal model. In addition, both maximum values of 10-g averaged SARs are same as 1.36 W/kg.

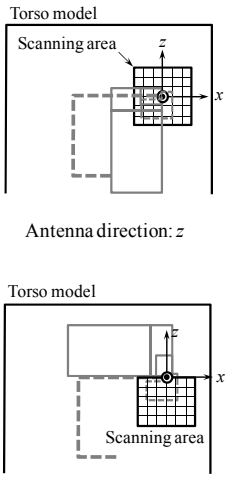

Figure 6. Scanning area of the mobile radio terminal model.

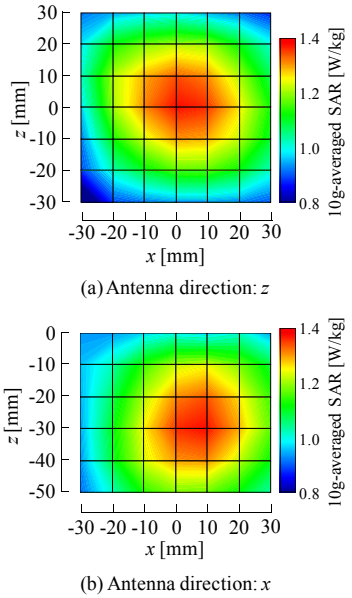

Figure 7. Calculated 10-g averaged SARs. The value of each crossing point corresponds the maximum 10-g averaged SAR in the calculated region, when the feeding point of the wireless radio terminal model was placed on this crossing point.

Table 2 shows comparison of the SAR values between with and without the pacemaker model, where the maximum 10-g averaged SAR value was observed. From the results, in the case of embedding the pacemaker model, the maximum value of 10-g averaged SAR is 30 % larger than that of without pacemaker model.

Figure 8 shows the SAR distributions around pacemaker model in both antenna directions. Here, SAR observation plane is *x*-*z* plane at the surface of the pacemaker housing (*y* =13 mm). The positions of wireless radio terminal model and pacemaker model are the points where the maximum 10-g average SAR was observed in Figs. 7 (a) and (b). From Fig. 8 (a), in the case of antenna direction *z*, high SAR region is observed at border of pacemaker housing and the region, where is the metallic case of the mobile radio terminal model faced (around *x* = -30 mm, *z* = -70 mm). Moreover, from Fig. 8 (b), in the case of antenna direction *x*, high SAR region is also observed at border of pacemaker housing and around the lead wire. They are because of the concentrate on electric field around the conductor.

In addition, SAR distributions under various implanted depth "*d*" are presented in Fig. 9. Here, the observation line is *y*-axis at *x* = -12 mm, *z* = -19 mm (center of pacemaker housing). According to Fig. 9, standing waves are observed between the torso surface and pacemaker model in all cases.

Figure 10 shows one of the examples of electric field distributions around the pacemaker model. From the results, it is observed that the dominant components of standing waves are *x* and *z*. The detail mechanism of the standing wave should be analysed as our further study.

IV. Conclusions

According to the results, the SAR around the conductor, which is implanted in the human body, increased. It is confirmed in [8] as well as our results. In fact, 10-g averaged SAR has been limited in less than 2 W/kg by the guideline on human exposure to electromagnetic fields in Japan. In addition, when the conductors were implanted into the human body, the guideline indicated that the possibility of the exposure below the guideline value might cause a local heating. Thus, the guideline value (i. e. 2 W/kg) was not applied in this case. However, as increasing number of pacemaker user, such a case must be applied to the guideline [9]. Therefore, the influences on SAR by the implanted conductors have to be investigated in detail [10].

Acknowledgment

The authors would like to thank Mr. Watanabe and Mr. Haga for their valuable help for numerical calculations.

TABLE II
Calculated SAR Values with and without Pacemaker Model

	Pacemaker model	
	with	without
10-g averaged SAR [W/kg]	1.36	1.04

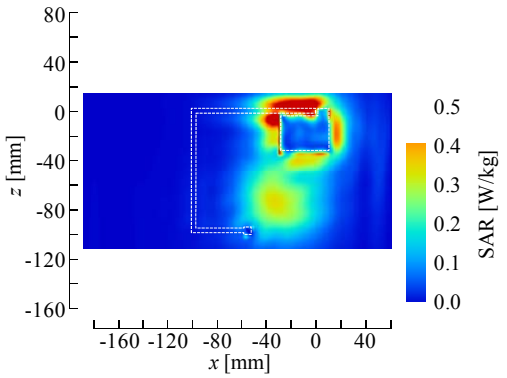

(a) Antenna direction: *z*

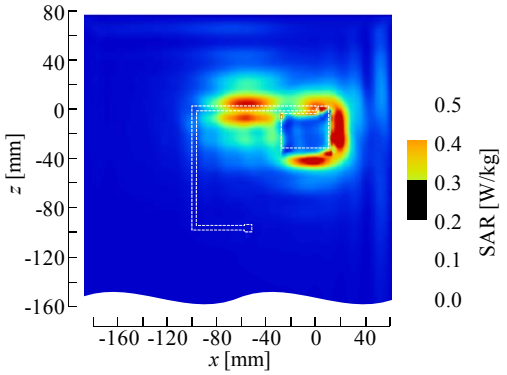

(b) Antenna direction: *x*

Figure 8. Calculated SAR distributions.

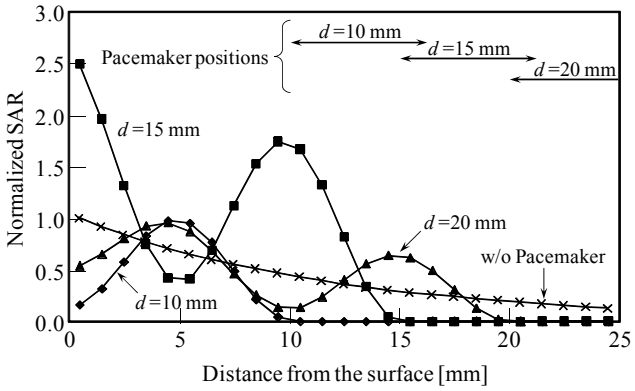

Figure 9. SAR profiles on *y* -axis at *x* =-12 mm, *z* =-19 mm (center of pacemaker housing). The values are normalized by maximum value of "without pacemaker model".

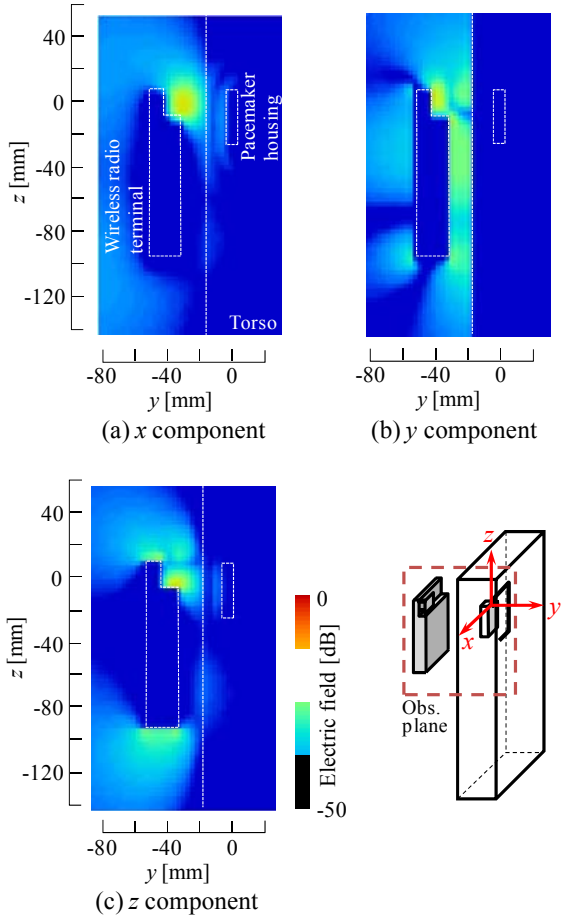

Figure 10. Calculated electric field distributions.

REFERENCES

[1] S. Stefan, LO. Fichte, and S. Dickmann, "EMC Modelling of Cardiac Pacemakers," in Electromagnetic Compatibility, 2007, -EMC Zurich 2007, 18th International Zurich Symposium, Sep. 2007.

[2] S. Hille, KF. Eichhorn, and KH. Gonschorek, "Determination of the interference voltage in implantable medical devices with bipolar electrodes," in Electromagnetic Compatibility -EMC Europe 2008 International Symposium, Sep. 2008.

[3] S. Schenke, F. Sabath, M. Clemens, and S. Dickmann, "Electromagnetic Interference Coupling into Cardiac Pacemaker Electrodes," in Electromagnetic Compatibility -EMC Europe 2008 International Symposium, Sep. 2008.

[4] "Guidelines on the Use of Radio communication Equipment such as Cellular Telephones -Safeguards for Electronic Medical Equipment- ," EMC Conference Japan, Electromagnetic Medical Equipment Study Group, 1997.

[5] J. Wang, O. Fujiwara, and T. Nojima, "A model for predicting electromagnetic interference of implanted cardiac pacemakers by mobile telephones," IEEE Transactions on Microwave Theory and Techniques, vol. 48, no. 11, pp. 2121-2125, Nov. 2000.

[6] C. Gabriel, "Compilation of the dielectric properties of body tissues at RF microwave frequencies," Brooks Air Force Technical Report AL/OE-TR-1996-0037, 1996.

[7] K. S. Yee, "Numerical solution of initial boundary value problems involving Maxwell's equation in isotropic media," IEEE Transactions on Antennas and Propagations, vol. AP-14, no. 3, pp. 302-307, May 1966.

[8] H. Virtanen, J. Huttunen, A. Toropainen, and R Lappalaiainen, "Interaction of mobile phones with superficial passive metallic implants," Physics in Medicine and Biology, vol. 50, pp. 2689-2700, 2005.

[9] C. R. Roy, "Rapporteur report: ICNIRP international workshop on EMF dosimetry and biophysical aspects relevant to setting exposure guidelines," Health Phyics, vol. 92, no. 6, pp. 658- 667, 2007.

[10] International Commission on Non-Ionizing Radiation Protection, "Exposure to high frequency electromagnetic fields, biological effects and health consequences (100 kHz-300 GHz) - review of the scientific evidence and health consequences," 2009.

978-1-61284-993-5/11/$26.00 ©2011 IEEE